arXiv:cond-mat/0609037v2 [cond-mat.mes-hall] 12 Jan 2007

Dirac and Normal Fermions in Graphite and Graphene: Implications to the Quantum Hall Effect

Igor A. Luk'yanchuk[1,2] and Yakov Kopelevich[3]

[1] *University of Picardie Jules Verne, Laboratory of Condensed Matter Physics, Amiens, 80039, France*
[2] *L. D. Landau Institute for Theoretical Physics, Moscow, Russia*
[3] *Instituto de Física "Gleb Wataghin", Universidade Estadual de Campinas, Unicamp 13083-970, Campinas, Sao Paulo, Brazil*

(Dated: February 4, 2008)

Spectral analysis of the Shubnikov de Haas (SdH) magnetoresistance oscillations and of the Quantum Hall Effect (QHE) measured in quasi-2D highly oriented pyrolytic graphite (HOPG) [Phys. Rev. Lett. 90, 156402 (2003)] reveals two types of carriers: normal (massive) electrons with Berry phase 0 and Dirac-like (massless) holes with Berry phase π. We demonstrate that recently reported integer- and semi-integer QHE for bi-layer and single-layer graphenes take place simultaneously in HOPG samples.

PACS numbers: 81.05.Uw, 71.20.-b

Observations of the quantum Hall effect (QHE) and magnetic-field-driven metal-insulator transition in quasi-2D highly oriented pyrolytic graphite (HOPG) [1, 2] indicate that much in the physics of graphite had been missed in the past and had triggered a considerable interest in graphite once again. Analyzing the quantum de Haas van Alphen (dHvA) and Shubnikov de Haas (SdH) oscillations in bulk HOPG samples we experimentally proved [3] that, besides the conventional electronic charge carriers with the massive spectrum $E = p^2/2m$, massless (2+1)-dimensional fermions (holes) with Dirac-like linear spectrum $E = \pm v|p|$ and non-trivial Berry phase π do exist in graphite. It is likely that these Dirac-type carriers are responsible for the strongly correlated phenomena predicted by theory [4, 5, 6]. The results of [3] were confirmed by the recent angle resolved photoemission spectroscopy (ARPES) experiments performed on HOPG [7, 8], that provide an unambiguous experimental evidence for coexistence of Dirac-like holes and normal (massive) electrons located at H and K poins of the Brillouin zone, respectively.

Very recently, remarkable progress in the technology of ultrathin films consisting of one [9, 10], two [11] or several [12] graphite monolayers (graphenes) was achieved. Analysis of unconventional half-integer QHE and Berry phase π of SdH oscillations in graphene led to the conclusion that charge carriers in graphene have the nature of Dirac-like massless fermions [9, 10]. At the same time, bilayer graphene demonstrates a new type of the integer QHE in which the last (zero-level) plateau is missing, and therefore the charge carriers are described by the chiral fermions having the Berry phase 2π and the energy spectrum is represented by two touching parabolas $E(p) = \pm p^2/2m$ [11].

In the present work we apply our filtering and phase analysis procedures [3] to analyze the SdH oscillations and the QHE effect in HOPG aiming to clarify how these effects correlate with those studied in single and bilayer graphene systems. In particular, we demonstrate that normal and Dirac-like fermions seen in the bulk graphite are responsible respectively for the integer and semi-integer precursors of the QHE. To check the independence of these conclusions on the windowing and frequency filtration cut-off we used an alternative, insensitive to filtration procedure method of two-dimensional phase-frequency analysis, described in detail in [3].

We analyze the field dependencies of the basal-plane resistance $R_{xx}(B)$ and the Hall resistance $R_{xy}(B)$ reported in Ref. [1] for the sample labeled as HOPG-3 (noting that the HOPG-UC sample, similar to HOPG-3, has been studied in Ref. [3]).

As seen from Fig. 1, $R_{xy}(B)$ demonstrates several QHE-like plateaus at high fields, also observed in various HOPG samples by other groups [13, 14]. However, unlike the conventional QHE, $R_{xx}(B)$ does not drop to zero at the positions of these plateaus. Only weak SdH oscillations $\Delta R_{xx}(B)$ [3] are seen superimposed on al-

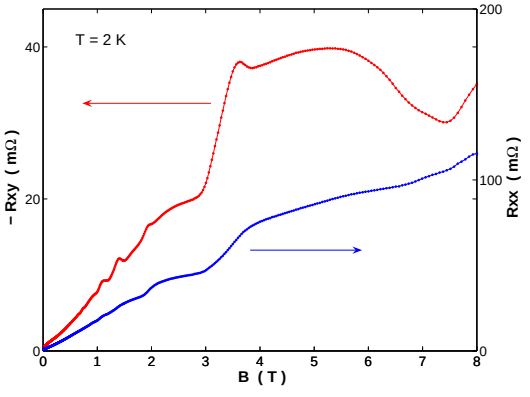

FIG. 1: Field dependence of basal-plane magnetoresistance $R_{xx}(B)$ and Hall resistance $R_{xy}(B)$ measured for the HOPG-3 sample with magnetic field B applied along the sample c-axis [1].

most linear $R_{xx}(B)$ dependence. This can be explained either by imperfection of the QHE itself or by the existence of a background resistance of unknown origin. It is interesting to note that QHE with similar behavior of $R_{xx}(B)$ has been reported for Bechgaard salts [15, 16] and for $(Bi_{1-x}Sb_x)_2Te_3$ layered semiconductors [17, 18].

Because quantum oscillations are periodic functions of the inverse field B^{-1}, the inverse-field spectral analysis is the appropriate tool to discriminate between different groups of carriers involved in oscillations. Fig. 2 presents the spectral intensity of SdH oscillations of the resistance $R_{xx}(B^{-1})$ and the Hall conductance $G_{xy}(B^{-1}) \equiv R_{xy}^{-1}(B^{-1})$, (in both cases polynomial background has been subtracted) together with analyzed in [3] spectral intensity of dHvA oscillations of magnetic susceptibility $\chi(B^{-1})$, ($\chi = dM/dB$).

Fig. 2 shows that two peaks in the susceptibility spectrum observed at 4.68T and at 6.41T are also resolved in the spectrum of $G_{xy}(B^{-1})$. The higher-frequency magnetoresistance peak manifests itself as the right-shoulder structure of $R_{xx}(B^{-1})$ spectrum. From comparative analysis of dHvA and SdH oscillations in [3] we identified these peaks as originating from normal (electrons) and Dirac (holes) carriers. Here, we re-affirm this conclusion in a different way, namely by means of the comparative analysis of longitudinal and Hall conductance oscillations, which is based on the separate study of the contributions from both types of carriers.

Fig. 3 (curves a and b) shows the raw data of $G_{xy}(B^{-1})$ and $\Delta R_{xx}(B^{-1})$ (after background signal subtraction) in which the normal electron contribution dominates in the magnetotransport quantum oscillations [3]. Extraction of the Dirac-like carriers signal from these data was the most challenging task that we performed

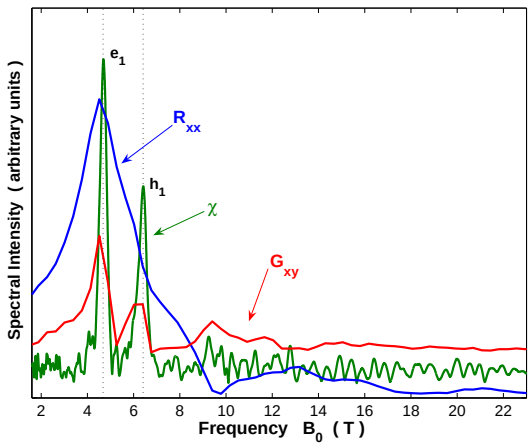

FIG. 2: Spectral intensity of SdH oscillations of magnetoresistance $|R_{xx}(B_0)|$ and of Hall conductance $|G_{xy}(B_0)|$ in HOPG-3 sample in comparison with dHvA oscillations of susceptibility $|\chi(B_0)|$ in HOPG-UC sample [3]. Peaks e_1 and h_1 correspond to the normal electrons and Dirac holes, respectively

by stop-band filtering of $G_{xy}(B^{-1})$, eliminating the frequency windows related to the electron spectral peak and

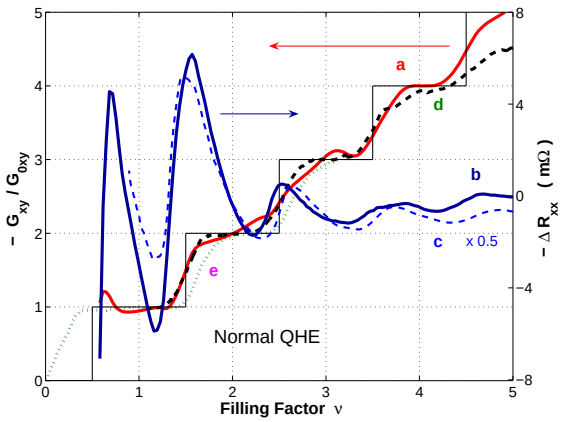

FIG. 3: Hall Conductance G_{xy} (solid line a) and $\Delta\sigma_{xx} \sim -\Delta R_{xx}$ (solid line b) for HOPG-3 sample as a function of the normalized "filling factor" $\nu = B_0/B$ (were $B_0 = 4.68T$ is the SdH oscillation frequency). Normal electrons give the dominant contribution in the quantum oscillations. The profile of $G_{xy}(\nu)$ is fitted by the integer QHE staircase; the minima of $\Delta\sigma_{xx}$ correspond to the QHE plateaus. Hall conductance is normalized on $G_{0xy} = 28\Omega^{-1}$ equal to the step between QHE plateaus. The results are compared with SdH oscillations in thick film of graphite (dashed line c) [13](having approximately the same $B_0 = 4.65T$) and with the QHE in bilayer graphene [11] obtained as a function of both magnetic field (dashed line d) ($\nu = B_0/B$, $B_0 = 27.8T$) and concentration (dotted line e) ($\nu = n/n_0$ with $n_0 = 1.7 \cdot 10^{12} cm^{-2}$ at $B = 20T$)

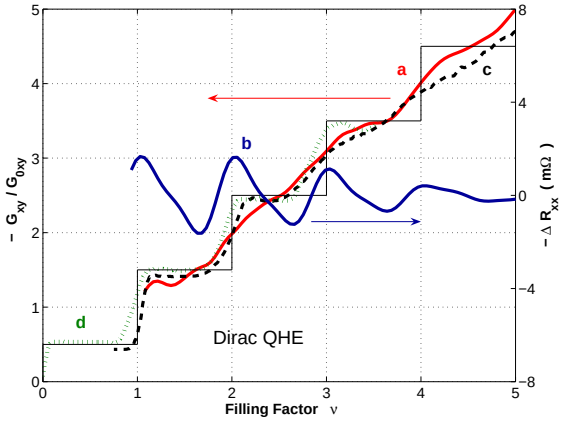

FIG. 4: Solid lines a and b : the same as in Fig. 3 (with $B_0 = 6.41T$, $G_{0xy} = 19\Omega^{-1}$) but after filtering elimination of the normal electrons contribution. The $G_{xy}(\nu)$ profile and positions of the minima in $\Delta\sigma_{xx} \sim -\Delta R_{xx}$ are coherent with the Dirac QHE staircase. The results are compared with the Dirac QHE in graphene monolayer obtained both as a function of magnetic field ($\nu = B_0/B$ with $B_0 = 6.67T$) (dashed line c) [10] and carrier concentration ($\nu = n/n_0$ with $n_0 = 1.5 \cdot 10^{12} cm^{-2}$ at $B = 14T$)(dotted line d) [9]

its harmonics (see Fig. 2) and using the pass-band filtering of $\Delta R_{xx}(B^{-1})$ with the corresponding hole frequency windowing. The resulting contributions from Dirac-like carriers are presented in Fig. 4 (curves a and b).

Note that the sign of ΔR_{xx} is reversed in order to present the oscillating part of the conductivity $\Delta\sigma_{xx}$, because in our case of $\rho_{xx} \gg \rho_{xy}$ and $\Delta\sigma_{xx}$ is related to ΔR_{xx} as:

$$\Delta\sigma_{xx} = \Delta\frac{\rho_{xx}}{\rho_{xx}^2+\rho_{xy}^2} \simeq -\frac{\Delta\rho_{xx}}{\rho_{xx}^2} \sim -\Delta R_{xx}. \qquad (1)$$

The situation is just opposite to the conventional QHE case with giant oscillations of $R_{xx}(B)$ when $\rho_{xx} \ll \rho_{xy}$ and σ_{xx} behaves in the same way as R_{xx}. Note also that the amplitude of SdH oscillations associated with Dirac-like fermions (Fig. 4, curve b) is three times smaller than that for normal carriers (Fig. 3, curve b).

To facilitate the comparative analysis of the results obtained for various graphite (graphene) samples, we present all the data as a function of the normalized filling factor $\nu = B_0/B$, where B_0 corresponds to the SdH oscillation frequency. The conductance G_{xy} is normalized by G_{0xy}, ($\simeq 28\Omega^{-1}$ for electrons and $19\Omega^{-1}$ for holes) corresponding to the step between subsequent QHE plateaus.

Fig. 3 (curve c) includes SdH oscillations reported for an $8\mu m$ thick HOPG sample taken from the inset of Fig. 4 in [13] after the polynomial background signal subtraction. The coincidence of the SdH oscillation frequency, phase and the asymmetric form of the signal with those measured in our HOPG sample suggests that the same Fermi surface electron pocket is responsible for SdH oscillations in both samples.

Before we proceed with the data analysis, we note that Landau Level (LL) quantization spectra for normal and Dirac-like carriers are different. In the normal carrier case the equidistant LLs $E_n = (e\hbar/m_\perp c)B(n+1/2)$ [19] are separated by the gap $E_0 = e\hbar B/2m_\perp c$ from $E = 0$ whereas in the Dirac-like case $E_n = \pm v\sqrt{2e\hbar Bn/c}$ [20], and the Lowest Landau Level (LLL) is located exactly at $E_0 = 0$. This leads to two important experimental consequences.

(i) SdH oscillations of conductivity [3]

$$\Delta\sigma_{xx}(B) \simeq -A(B)\cos[2\pi(\frac{B_0}{B}-\gamma+\delta)] \qquad (2)$$

(where $A(B)$ is the non-oscillating amplitude) acquire the phase factor either $\gamma = 1/2$ or $\gamma = 0$ for normal and Dirac carriers, respectively. The additional phase factor δ governed by the curvature of Fermi surface is quite small: $|\delta| < 1/8$ (in 2D $\delta = 0$) and can be neglected.

(ii) QHE plateaus occur either in integer (normal carriers) or in semi-integer (Dirac fermions) way and can be expressed via the phase factor γ as [21, 22]:

$$G_{xy} = \mu g_s\frac{e^2}{h}(n+\frac{1}{2}-\gamma) \qquad (3)$$

where $\mu = \mp 1$ for electrons/holes, and g_s is the (iso)-spin degeneracy factor.

The phase factor γ is defined for an arbitrary spectrum $E(p)$ by the quasiclassical quantization condition of the Fermi surface cross-section $S(E_f) = (n+\gamma)2\pi eB/\hbar c$ ($n \gg 1$). This factor is uniquely related to the topological Berry phase $\Phi_B = k\pi$ acquired by a fermion, moving around $S(E_f)$ [23]: γ equals either 1/2 for even k (normal carriers) or 0 for odd k (Dirac-like fermions). For example, the two-parabola spectrum of bilayer graphite $E(p) = \pm p^2/2m_\perp$ is quantized in magnetic field as: $E_n = \pm(e\hbar/m_\perp c)B\sqrt{n(n-1)}$ [24]. This gives an unconventional doubly degenerate LLL with $E_0 = E_1 = 0$ but for higher n the system recovers the behavior of normal carriers having $\gamma = 1/2$ (with $n \to n-1$ in (3)).

We obtain the phase factors γ and δ by plotting the inverse field values at conductivity oscillation maxima (minima) as a function of their number (number - 1/2), as shown in Fig. 5. The linear extrapolation of data points to $B^{-1} = 0$ unambiguously determines the phase factors: $\gamma = 1/2$, $\delta \simeq -1/8$ for data depicted in Fig. 3 (curve b) and $\gamma = 0$, $\delta = 0$ for data shown in Fig. 4 (curve b). Thus, we identify here normal (3D) and Dirac-like (2D) charge carriers in agreement with our previous results obtained for HOPG-UC sample [3].

Curves (a) in Figs. 3 and 4 provide evidence for the staircase behavior (quantization) of G_{xy} for both normal and Dirac-like fermions. As expected for QHE regime, the minima in longitudinal conductivity σ_{xx} coincide with the plateau positions in G_{xy}.

In the case of normal carriers , Fig. 3 (curve a), the quantization of G_{xy} corresponds to the integer QHE, as

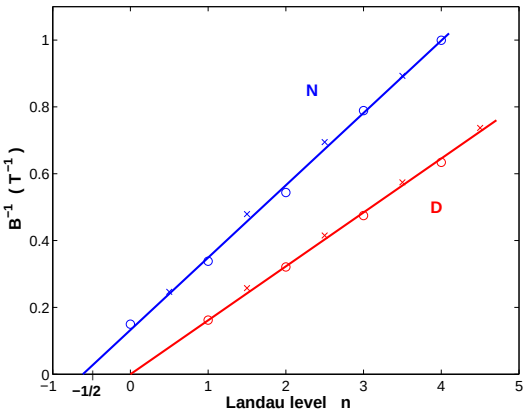

FIG. 5: Values of B^{-1} for the normal (N) and Dirac-like (D)charge carriers at which n*th* Landau level crosses the Fermi level. These values are found as maxima (o) in the SdH oscillations of magnetoconductivity $\Delta\sigma_{xx}(B)$. The minima positions (x) in $\Delta\sigma_{xx}(B)$ are shifted by 1/2 to the left. Linear extrapolation of the data to $B^{-1} = 0$ (solid lines) allows for the phase factor ($-\gamma+\delta$, Eq. (2)) definition: $\gamma = 1/2$, $\delta \simeq -1/8$ for normal electrons and $\gamma = 0$, $\delta = 0$ for Dirac-like holes.

follows from Eq. (3) for $\gamma = 1/2$. In the same Fig. 3 we presented the QHE staircases of σ_{xy}, reported in [11] for bilayer graphite as function of both inverse field B^{-1} (Fig. 3, curve d) and carrier concentration n (Fig. 3, curve e). The scales of B^{-1} and n were normalized to the corresponding oscillation periods of σ_{xx}. The Hall conductivity was normalized to the step between subsequent plateaus in $\sigma_{xy}(B)$. The comparative analysis indicates that all three dependencies, i. e. $G_{xy}(B^{-1})$ for HOPG, $\sigma_{xy}(B^{-1})$ and $\sigma_{xy}(n)$ for bilayer graphene are equally well fit to the integer QHE theory with $\gamma = 1/2$. We stress, however, that our data don't allow us to distinguish between the conventional integer QHE with Berry phase 0 and the chiral one with Berry phase 2π, proposed for bilayer graphite [11]. This is because both models imply $\gamma = 1/2$ and the same integer QHE staircase at LL $n > 1$. The only difference between them is the absence of zero level plateau for chiral fermions whose (non)existence we cannot verify at the moment.

It is interesting to note that the absolute values of Hall steps $\Delta\rho_{xy}^{-1}$, estimated (similar to [1]) as $(10\,\mathrm{k}\Omega/\Box)^{-1}$ for electrons and $(15\,\mathrm{k}\Omega/\Box)^{-1}$ for holes are approximately equal to the two-spin degenerate QHE step $2e^2/h \simeq (12.9\,\mathrm{k}\Omega/\Box)^{-1}$ ($g_s = 2$ in (3)) and are twice as small as the two-spin two-valley degenerate QHE step with $g_s = 4$, reported for graphene [9, 10] and bilayer graphite [11].

To conclude, the results reported in this letter give new insight on the behavior of Dirac and normal fermions in graphite. Namely, we demonstrate the coexistence of QHE precursors associated with normal electrons and Dirac-like holes. To the best of our knowledge this is the first observation of the simultaneous occurrence of integer and semi-integer quantum Hall effects.

This work was supported by Brazilian scientific agencies FAPESP, CNPq, CAPES, and French agency COFECUB. We thank to Prof. M. G. Karkut for the useful discussions.

[1] Y. Kopelevich, J.H.S. Torres, R.R. da Silva, et al., Phys. Rev. Lett. **90**, 156402 (2003).

[2] Y. Kopelevich, V. V. Lemanov, S. Moehlecke, and J. H. S. Torres, Phys. Solid State **41**, 1959 (1999); [Fiz. Tverd. Tela (St. Petersbrug) **41**, 2135 (1999)].

[3] I. A. Luk'yanchuk and Y. Kopelevich, Phys. Rev. Lett. **93**, 166402 (2004).

[4] J. González, F. Guinea, and M. A. H. Vozmediano, Phys. Rev. Lett. **77**, 3589 (1996).

[5] D. V. Khveshchenko, Phys. Rev. Lett., **87**,206401 (2001); ibid. **87**, 246802 (2001).

[6] E. V. Gorbar, V. P. Gusynin, V. A. Miransky, and I. A. Shovkovy, Phys. Rev. **B66**, 045108 (2002).

[7] S. Y. Zhou, G.-H. Gweon and A. Lanzara, Annals of Physics **321**, 1730(2006).

[8] S. Y. Zhou, G.-H. Gweon, J. Graf et al., Nature Physics **2**, 595 (2006).

[9] K. S. Novoselov, A. K. Geim, S. V. Morozov et al., Nature (London) **438**, 197 (2005).

[10] Y. Zhang, Y.-W. Tan, H. L. Stormer, and Philip Kim, Nature (London) **438**, 201 (2005).

[11] K. S. Novoselov, E. McCann, S. V. Morozov et al. Nature Physics **2**, 177 (2006).

[12] S. V. Morozov, K. S. Novoselov, F. Schedin et al. Phys. Rev. **B72**, 201401(R) (2005).

[13] K. S. Novoselov, A.K. Geim, S.V. Morozov et al., Prteprint cond-mat/0410631 (2004).

[14] Y. Niimi, H. Kambara, T. Matsui et al., Physica **E34**, 100 (2006) .

[15] S. T. Hannahs, J. S. Brooks, W. Kang et al., Phys. Rev. Lett. **63**, 1988 (1989).

[16] D. Poilblanc, G. Montambaux, M. Héritier, and P. Lederer, Phys. Rev. Lett. **58**, 270-273 (1987).

[17] D. Elefant, G. Reiss, and Ch. Baier, Eur. Phys. J. **B4**, 45 (1998).

[18] M. Sasaki, N. Miyajima, H. Negishi et al., Physica **B298**, 510 (2001).

[19] L. D. Landau, and E. M. Lifschitz, Quantum Mechanics (Non-Relativistic Theory), Butterworth-Heinemann (1981).

[20] E. M. Lifshitz, L. P. Pitaevskii and V. B. Berestetskii, Quantum Electrodynamics, Butterworth-Heinemann(1982).

[21] V. P. Gusynin and S. G. Sharapov, Phys. Rev. Lett. **95**, 146801(2005).

[22] N. M. R. Peres, F. Guinea, and A. H. Castro Neto, Phys. Rev. **B73**, 125411 (2006).

[23] G. P. Mikitik and Yu.V. Sharlai, Phys. Rev. Lett. **82**, 2147 (1999).

[24] E. McCann and V. I. Fal'ko, Phys. Rev. Lett. **96**, 086805 (2006).